Diagnostic and Interventional Imaging 102 (2021) 329–332

Letter/*Research, New developments & Artificial Intelligence*

Feasibility of human vascular imaging of the neck with a large field-of-view spectral photon-counting CT system

Keywords:
Computed tomography scanners X-ray
Computed tomography angiography
Contrast materials iodine compounds
Imaging diagnostic
Photon-counting detectors

Dear Editor,

A new generation of computed tomography (CT) systems featuring energy-resolved photon-counting detectors (PCDs), spectral photon-counting CT (SPCCT), yielded promising results in the last years, especially regarding high spatial resolution and low dose imaging that have been the key focus of previous investigations. Nonetheless, the spectrum of capabilities of SPCCT at its full potential is much broader [1]. SPCCT provides photon by photon energy-dependent information sorted in multiple energy bins, improving the sampling of the transmitted spectrum leading to a more accurate energy resolution and material decomposition [2]. While the potential of this spectral data has already been demonstrated on dual-energy systems with energy-integrating detectors (EID), particularly for vascular and perfusion imaging [3,4], information is lacking about these applications with SPCCT.

In this letter, we wished to report our preliminary in-vitro and in-vivo experience with the multi-energy resolving capabilities of a new large field of view (FOV) prototype SPCCT system adapted to clinical use.

The SPCCT system is a large FOV (500 mm in-plane) prototype equipped with PCD, the technical characteristics of which are provided in Table 1. Each channel offers pulse-height discrimination with five controllable energy thresholds. The current full spectral image reconstruction chain follows a two-step approach. First, the photon counts from the five energy bins are used to provide conventional CT images. Thereafter, spectral images are derived by performing projection domain material decomposition into two or three basis materials using a forward projection model (per detector), literature energy dependent attenuation data, and a maximum likelihood based algorithm taking into account the Poisson noise distribution of the measured data [5]. Pile-up and precise detector response corrections are based on calibration data. In a subsequent step, each single basis material is reconstructed separately using a filtered back-projection reconstruction algorithm [6].

The SPCCT system was first tested using phantoms. Ten 1.5 mL polypropylene tubes with known pre-calibrated concentrations of iodine (0.1 to 15 mg/mL) and one control tube were scanned in an anthropomorphic thorax phantom (QRM thorax phantom, GmbH) at 120 kVp and 200 mAs in axial mode. Nominal energy thresholds were set at 30, 51, 62, 72, 81 keV, as optimized for dual contrast agent imaging (*i.e.*, for iodine plus Gd or Au k-edge imaging, since, for instance, the k-edge value of Gd is of 50.2 keV) [1,7]. Conventional and material decomposition (iodine-water basis) images were reconstructed using 2×8 downsampling on the sinograms, 200 mm FOV, 512×512 mm^2 matrix size, 2 mm slice width and a Detailed 2 filter (Fig. 1). Equal-sized circular regions-of-interest were manually placed in the middle of each tube to measure iodine concentrations. Linear regression analysis showed strong correlation ($R^2 = 0.99$; slope = 0.94; and offset on the y-axis = 0.03) between prepared and measured concentrations (Fig. 1, Table 2). The intraclass correlation coefficient (ICC), calculated with a two-way mixed effects model, was very good (ICC = 1; 95% confidence interval: 0.99–1) [8].

For in vivo vascular imaging of the neck, a standard carotid artery protocol was employed in one patient. A total of 40 mL of iodinated contrast agent (iomeprol, Iomeron®400, Bracco Imaging) was injected at 4 mL/s followed by a saline flush of 20 mL. Conventional, material decomposition (iodine-water basis) images and virtual mono-energetic (VME) images at 40, 50, 60, 70 keV were reconstructed. VME were generated using our in-house research platform based on a linear combination of the iodine/water basis material images. VME displayed an increasing mean attenuation value with decreasing keV (312, 424, 605 and 896 HU at 70, 60, 50 and 40 keV respectively) and iodine maps yielded an objective

Table 1
System parameters of the clinical prototype spectral photon counting CT system.

Parameter	Large field of view SPCCT
Platform	Philips iCT®
Supported scan modes	Axial, axial multicycles, helical
Tube voltages (kVp)	80, 100, 120, 140
Tube currents (mA)	10–500
X-ray filter	Half value layer (HVL) = 7.1 ± 0.7 (SD) mm at 120 kVp
Focal spot (mm × mm)	0.6 × 0.7 (dual focal spots)
Gantry rotation (s)	0.33, 0.4, 0.5, 0.75, 1.0
Projections per rotation	2400
Number of focal spots	2
Z-coverage in isocenter (mm)	17.5
Number of detectors per row/column	64/1848
Field of view (mm)	500
Pixel pitch (μm × μm)	270 × 270 mm^2 at isocenter
Readout electronic	Philips ChromAIX2
Number of energy thresholds	5
Sensor material	Cadmium Zinc Telluride, 2-mm thickness

SPCCT: Spectral photon counting CT; FOV: Field of view; SD: Standard deviation.

https://doi.org/10.1016/j.diii.2020.12.004

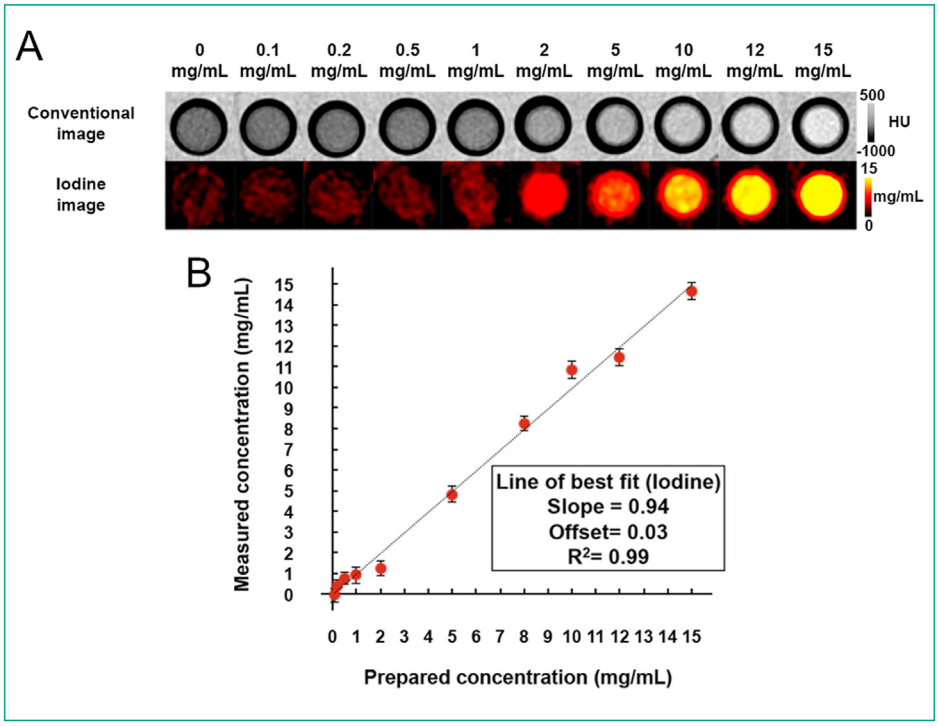

Fig. 1. A: In vitro conventional and iodine material decomposition images: Iodine image shows material specific increase in signal (from 0.1 to 15 mg/mL of iodine), without signal from the surrounding phantom material (displayed in the corresponding conventional image). B: linear regression analysis shows strong correlation between prepared (x-axis) and measured (y-axis) concentrations of iodine.

Table 2
SPCCT iodine quantification of tubes using an anthropomorphic thorax phantom.

	Tube 1	Tube 2	Tube 3	Tube 4	Tube 5	Tube 6	Tube 7	Tube 8	Tube 9	Tube 10
[C°] prepared	0.1	0.2	0.5	1	2	5	8	10	12	15
[C°] measured	0.1	0.2	0.5	0.8	1.8	4.9	7.8	10.1	11	13.9
SEM	0.3	0.3	0.3	0.3	0.4	0.3	0.3	0.4	0.4	0.5

[C°]: concentration in mg/Ml. SEM: standard error of the mean; SPCCT: spectral photon counting CT.

measurement of 12 mg/mL of iodine within the common carotid (Fig. 2). The same patient had a stenosis of the vertebral artery, due to osteoarthritis. The 3.58 × 0.7 mm lumen of the artery (Fig. 2) was clearly depicted thanks to the seemingly complete absence of artifacts next to bones.

In this pilot study, phantom analyses showed strong linear correlation (R^2 = 0.99) between measured and prepared iodine concentrations in line with results obtained with the former small FOV SPCCT system [7]. However, linear regression analysis showed a minor underestimation of iodine concentrations in the absence of offset correction, explicable by unresolved limitations of PCDs such as photon scattering and pile-up. In-vivo carotid images demonstrated, for the first time on a full FOV SPCCT system, visual variations in contrast on VME images and quantification capabilities. These qualitative and quantitative spectral features have direct applications in clinical tasks enabling variable iodine to soft tissue contrast and accurate quantification of iodine concentrations. Combined with high spatial resolution and artifact reduction, spectral capabilities define SPCCT as a major tool in the future of cardiovascular imaging. Further investigations are needed focusing on the clinical application of these contrast agent imaging features as compared to dual-energy EID systems. Moreover, future advancements in reconstruction algorithms specifically adapted to multiple energy bins, including noise suppression techniques, are expected to help further improve spectral resolution.

Ethical approval and informed consent

The authors declare that the work described has been carried out in accordance with the Declaration of Helsinki of the World Medical Association revised in 2013 for experiments involving humans. The authors declare that this report does not contain any personal information that could lead to the identification of the patient.

Funding

This work was performed within the framework of the EU's Horizon 2020 research and innovation program under the grant agreement No. 633937(grant recipient: Philippe Douek).

Author contributions

All authors attest that they meet the current International Committee of Medical Journal Editors (ICMJE) criteria for Authorship.

Credit (Contributor Roles Taxonomy)

Sara Boccalini: Conceptualization, Methodology, Formal analysis, Investigation, Writing - Original Draft, Writing–Review

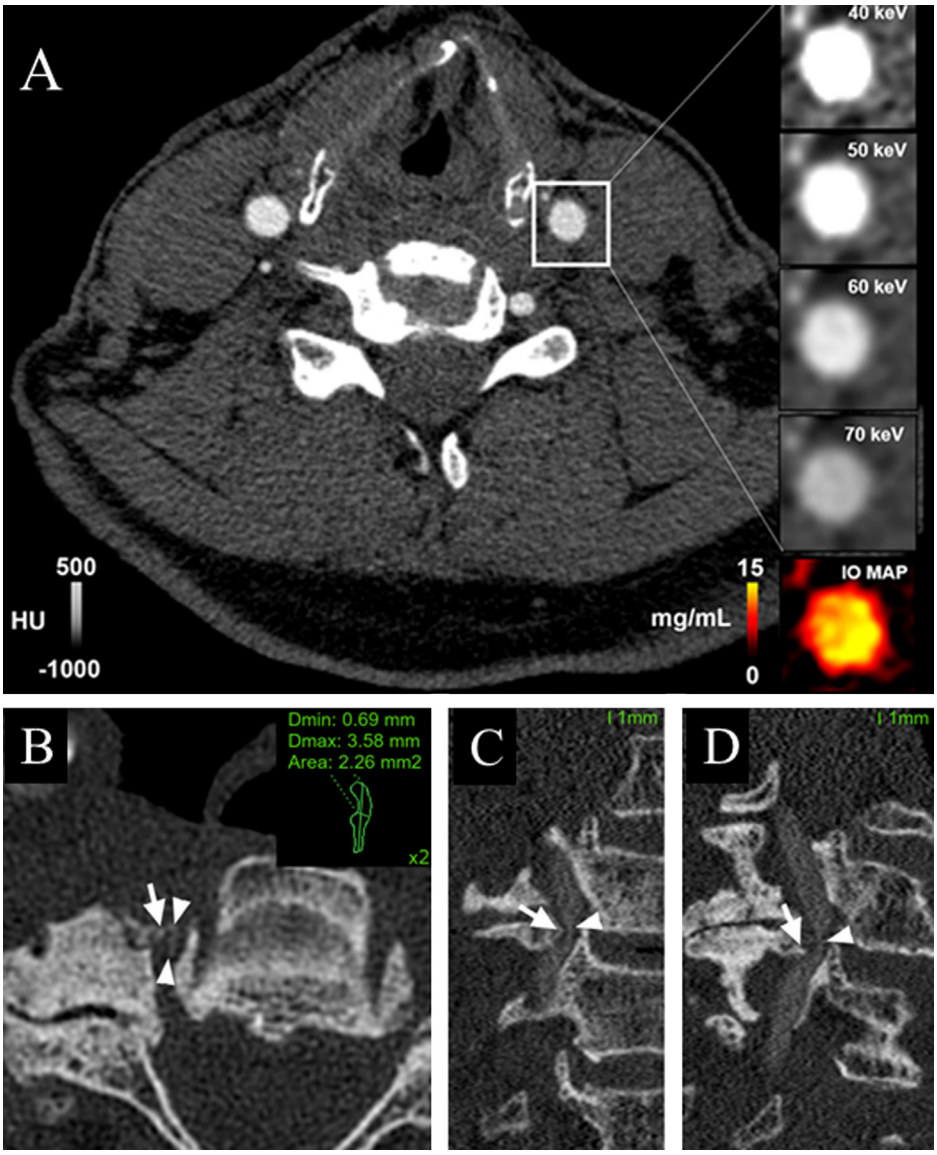

Fig. 2. In vivo arterial phase image of the carotid arteries. A: full field-of-view conventional image with zoomed virtual mono-energetic (VME 40, 50, 60, and 70 keV) and iodine material decomposition images of the left common carotid artery. B, C and D: axial (B) and multiplanar reconstructed images (C, D) demonstrate presence of osteophytes (arrows) responsible for severe stenosis of right vertebral artery (arrowheads) at the level of C4-C5. The insert in B shows diameters (D_{min} and D_{max}) of residual patent arterial lumen.

and Editing. Salim Si-Mohamed: Conceptualization, Methodology, Formal analysis, Investigation, Writing - Original Draft, Writing–Review and Editing. Riham Dessouky: Validation, Formal analysis, Investigation, Writing–Review and Editing. Monica Sigovan: Validation, Formal analysis, Investigation, Writing–Review and Editing. Loic Boussel: Supervision, Project administration, Writing–Review and Editing. Philippe Douek: Supervision, Project administration, Writing–Review and Editing, Funding acquisition.

Acknowledgements

We thank Yoad Yagil, Lahoud Elias, Philippe Coulon, Klaus Erhard, Alain Vlassenbroek, Thomas Broussaud and Pierre-Antoine Rodesch for their global support.

Disclosure of interest

The authors declare that they have no competing interest.

References

[1] Si-Mohamed S, Boussel L, Douek P. Clinical perspectives of spectral photon-counting CT. In: Tagushi K, Blevis I, Iniewski K, editors. Spectral, photon counting computed tomography: technology and applications. Taylor & Francis: CRC Press; 2020. p. 97–116.
[2] Taguchi K, Iwanczyk JS. Vision 20/20: single photon counting x-ray detectors in medical imaging. Med Phys 2013;40:100901.
[3] Si-Mohamed S, Moreau-Triby C, Tylski P, Tatard-Leitman V, Wdowik Q, Boccalini S, et al. Head-to-head comparison of lung perfusion with dual-energy CT and SPECT-CT. Diagn Interv Imaging 2020;101:299–310.
[4] Jamali S, Michoux N, Coche E, Dragean CA. Virtual unenhanced phase with spectral dual-energy CT: is it an alternative to conventional true unenhanced phase for abdominal tissues? Diagn Interv Imaging 2019;100:503–11.
[5] Schlomka JP, Roessl E, Dorscheid R, Dill S, Martens G, Istel T, et al. Experimental feasibility of multi-energy photon-counting K-edge imaging in pre-clinical computed tomography. Phys Med Biol 2008;53:4031–47.
[6] Heuscher D, Brown K, Noo F. Redundant data and exact helical cone-beam reconstruction. Phys Med Biol 2004;49:2219–38.
[7] Si-Mohamed S, Bar-Ness D, Sigovan M, Tatard-Leitman V, Cormode DP, Naha PC, et al. Multicolour imaging with spectral photon-counting CT: a phantom study. Eur Radiol Exp 2018;2:34.
[8] Benchoufi M, Matzner-Lober E, Molinari N, Jannot AS, Soyer P. Interobserver agreement issues in radiology. Diagn Interv Imaging 2020;101:639–41.

Sara Boccalini [a,b,1,*]
Salim Si-Mohamed [a,b,c,1]
Riham Dessouky [d]
Monica Sigovan [c]
Loïc Boussel [a,b,c]
Philippe Douek [a,b,c]

[a] *Department of Cardiovascular and Thoracic Radiology, Hospices Civils de Lyon, 69002 Lyon, France*

[b] *University Claude-Bernard Lyon 1, 69100 Villeurbanne, France*

[c] *University Claude-Bernard Lyon 1, CREATIS, CNRS UMR 5220, INSERM U1206, INSA-Lyon, 69100 Villeurbanne, France*

[d] *Radiology Department, Faculty of Medicine, Zagazig University, 44519 Zagazig, Egypt*

[*] Corresponding author at: Department of Cardiovascular and Thoracic Radiology, Hospices Civils de Lyon, 69002 Lyon, France.
E-mail address: sara.boccalini@chu-lyon.fr (S. Boccalini)

[1] First authors with equal contribution.